

Bayesian Restoration of Medical X-Ray Digital Images

RADU MUTIHAC, MARC M. VAN HULLE
Laboratorium voor Neuro- en Psychofysiologie
Katholieke Universiteit Leuven
Campus Gasthuisberg, Herestraat 49, B-3000 Leuven
BELGIUM
{radu.mutihac, marc.vanhulle}@med.kuleuven.ac.be

Abstract: - Image entropy as prior in Bayesian inference was applied to the restoration of X-ray digital images with additive zero mean Gaussian distributed noise. An iterative algorithm based on a conjugate gradient method with numerical evaluation of partial derivatives was developed to efficiently minimize the potential function associated to any positive, additive distribution. The correlation matrix of the errors, both in the data acquisition and the modeling process, was built up and used as prior in Bayesian approach. Digitized and digitally acquired X-ray mammograms were subject of comparative analyses before and after running the algorithm. All output images displayed better overall quality as compared with their input counterparts in terms of contrast, signal to noise ratio, and visibility of details. No artifacts were detected by all means as being introduced by the entropic method, which theoretically ensures the least biased and structureless output image restoration.

Key-Words: - Bayesian inference, Maximum entropy principle, Inverse problem, X-ray digital image

1 Introduction

In many areas like data analysis, signal processing, and neural networks, a common task is to find an adequate representation of multivariate data for subsequent processing and interpretation. Linear transforms are often invoked due to their computational and conceptual simplicity. Despite of their sophistication and diversity, the numerical methods generally used to convert experimental data into interpretable images and spectra heavily rely on straightforward transforms, such as the Fourier transform, or quite elaborated emerging classes of transforms like wavelets [1] [2], wedgelets [3], ridgelets [4], and so forth. Yet experimental data are necessarily incomplete and noisy due to the limiting constraints of digital data recording and the finite acquisition time. The main drawback of these transforms is that defects in the data are directly transferred into the transform domain along with the genuine signals. The traditional approach to data processing in the transform domain is to ignore any known imperfections in the data, set to zero any unmeasured data points, and then proceed as if data were perfect. A different approach based on maximum entropy (ME) principle is to proceed from the frequency domain to the time domain. In data analysis, ME techniques are generally used to restore positive distributions, such as images and spectra, from blurred, corrupted or, generally, from imperfect data. ME methods may be developed on axiomatic foundations based on the

probability calculus, which itself has a special status as the only internally consistent language of inference [5]. Within its framework, positive distributions ought to be assigned probabilities that are based on the *entropy* of these distributions.

2 The Inverse Problem of Image Restoration

The methods used in image restoration are oriented towards modeling the image degradations and applying an inverse procedure to obtain a reliable approximation of the original scene.

If a digital image made out of N pixels is represented as sequence of positive numbers $f_n, n = 1, 2, \dots, N$ with corresponding proportions

$$p_n = f_n / \sum_{n=1}^N f_n,$$

then the axioms of probability are satisfied. Since the *configurational* structure of the images satisfies these axioms then the concept of *image entropy* may be introduced [6]. If we consider a complete collection of images corresponding to all possible intensity distributions, then measurements act as a filter over the collection by restricting our attention to the images that satisfy the data with any conceivable constraints (noise). Among these, a natural choice may be the one that could have arisen in the maximum number of ways, depending on our counting rule. By maximizing the entropy, the smoothest and most uniform distribution among the set of all admissible distributions is selected as the most featureless possible image. ME restoration allows to associate error bars on the retrieved

images which provides means to assess quantitatively and objectively the reliability of the extracted features. Furthermore, we are able to assess different variants of ME and give quantitative comparison [7].

The methods used in image restoration are oriented towards modeling the image degradations and applying an inverse procedure to obtain a reliable approximation of the original scene. Linear transforms encompass a large class of physical experiments [8]. In general, for an image with true continuous light intensity distribution $f(\mathbf{t})$, the measured image light intensity distribution $g(s)$ is given by the convolution equation

$$g(s) = \int_{-\infty}^{+\infty} r(s, \mathbf{t}) \cdot f(\mathbf{t}) \cdot d\mathbf{t} + e \quad (1)$$

where $r(s, \mathbf{t})$ is the space invariant *blurring function* (PSF) of the imaging system. It is nevertheless assumed that the *observed noise* e is independent of the function f . The inverse problem may be stated as to determine a *unique* and *stable* solution, say $\tilde{f}(\mathbf{t})$, representing the unknown function $f(\mathbf{t})$ by using the measured values $g(s)$ of the data. This is a typically *ill-posed* problem, in the sense that, generally, there are infinitely many solutions $f(\mathbf{t})$ consistent with the same data $g(s)$ and comply with the errors.

Practically, in a physical experiment $g(s)$ is observed on a finite set of isolated points s_m , $m = 1, 2, \dots, M$ in the data space D

$$g_m = g(s_m) = \int_D f(\mathbf{t}) \cdot r(\mathbf{t}, s_m) \cdot d\mathbf{t} + e(s_m) = \int_D f(\mathbf{t}) \cdot r_m(\mathbf{t}) \cdot d\mathbf{t} + e_m, \quad m = 1, 2, \dots, M \quad (2)$$

Furthermore, the statement should be correct only if the discretization is performed properly, i.e., each component g_m , $m = 1, 2, \dots, M$ of $g(s)$ measures a distinct aspect f_n , $n = 1, 2, \dots, N$ of $f(\mathbf{t})$ through its own linear response kernel $r_m(\mathbf{t})$, $m = 1, 2, \dots, M$, and with its own additive measuring error e_m , $m = 1, 2, \dots, M$. For a dense set of N discrete points t_n , $n = 1, 2, \dots, N$, which are sufficiently evenly spaced so that neither $f(\mathbf{t})$ nor $r_m(\mathbf{t})$, $m = 1, 2, \dots, M$ vary significantly between t_{n-1} and t_{n+1} , the components g_m may be put in a quadrature-like form

$$g_m = \sum_{n=1}^N R_{mn} f_n + e_m, \quad m = 1, 2, \dots, M \quad (3)$$

The above expression can be put in a matrix form $\mathbf{g} = \mathbf{R}\mathbf{f} + \mathbf{e}$, where \mathbf{R} is a matrix of size $M \times N$ having the components $R_{mn} = r_m(t_n) \cdot (t_{n+1} - t_{n-1})/2$. Though the number N of unknown pixel values, which we wish to determine, may equal to the number M of the observed values, the direct solution of the problem by inverting the matrix \mathbf{R} rarely works. This is the consequence of either \mathbf{R} being *singular* or *ill-conditioned*, or else, because the solution may include negative pixel values due to the unknown noise e . In fact, the finer the discretization of the continuous functions is, the more ill-conditioned \mathbf{R} [9].

Regularization theory deals with solving ill-posed or ill-conditioned problems through the analysis of an associated *well-posed* problem, whose solution is supposed to yield meaningful answers and approximations to the *ill-posed* problem. The *well-posed* inverse problem of image restoration may be formulated by asking for some reliable estimate \tilde{f} to the exact solution f , given the measured sample data \mathbf{g} , the space invariant PSF of the imaging system \mathbf{R} , and some information about the errors e , such as their covariance matrix

$$\mathbf{C} = \|C_{ij}\|_{i,j=1,2,\dots,M}$$

2.1 Image entropy

Any positive, additive image can be directly identified with a probability distribution. However, the correct definition of the entropy associated to an image and the particular mathematical function to describe it is still a question of debate [10].

As a prerequisite to apply Bayes' theorem, we must first use some other principle to translate the available information into numerical values. By *applying* the ME principle we mean *assigning* a probability distribution $\{p_n\} = \{p_1, p_2, \dots, p_N\}$ on some *hypothesis space* (i.e., all admissible images) by the criterion that it shall maximize some form of *entropy*, subject to constraints that express properties we wish the distribution to have, but are not sufficient to determine it. Entropy is used as the criterion for resolving the ambiguity remaining when we have stated all the constraints we are aware of. ME methods do not require for input numerical values of any probabilities on the image space, rather they assign numerical values to our information as expressed by our choices of image space and constraints. Among the probability

distributions that satisfy these constraints, the ME principle selects the one that maximizes the entropy. In our approach, we derived the image entropy form based on the fair reason that each quanta had an equal *a priori* chance of being in any pixel and counting the ways for getting a particular image configuration \mathbf{f} , which lead to

$$-\sum_{n=1}^N f_n \cdot \ln \frac{f_n}{U} = -U \sum_{n=1}^N p_n \cdot \ln p_n = S(\mathbf{f}) \quad (4)$$

where U stands for all recorded quanta that form the image. The above expression stands for the *entropy of an image*, which is not the same as the *thermodynamic entropy* of a beam of photons, nor is the same as the *information entropy* introduced by Shannon [11] in statistics!

2.2 Bayesian Inference

Bayesian approach does not specify any particular choice of prior. The entropic prior was argued by Skilling [18]. Given some background knowledge I , then Bayesian ME *prior* $Pr(\mathbf{f}/I)$ for a macroscopic state \mathbf{f} with entropy $S(\mathbf{f})$ is postulated as proportional to $\exp S(\mathbf{f})$, that is

$$Pr(\mathbf{f}/I) \propto \exp S(\mathbf{f}) = \exp \left(-\sum_{n=1}^N f_n \cdot \ln p_n \right) \quad (5)$$

Whatever prior is used, it clearly affects the amount by which the restoration is offset from the true image. The extent of this biasing effect depends on the relative weights of the *prior* $Pr(\mathbf{f}/I)$ and *likelihood* $Pr(\mathbf{g}/\mathbf{f}/I)$ in the expression of the *posterior* probability $Pr(\mathbf{f}/\mathbf{g}/I)$. Bayes' theorem combines the first two knowledge states and yields the posterior probability distribution law representing our updated state of knowledge of the solution

$$Pr(\mathbf{f}/\mathbf{g}/I) = \frac{Pr(\mathbf{g}/\mathbf{f}/I) \cdot Pr(\mathbf{f}/I)}{Pr(\mathbf{g}/I)} \quad (6)$$

where the evidence $Pr(\mathbf{g}/I)$ plays merely the role of a normalization constant of no significance in any variational problem, yet meaningful in model ranking.

2.3 The potential function

For the widely spread case of linear experiments with additive Gaussian noise $\mathbf{g} = \mathbf{R}\mathbf{f} + \mathbf{e}$ the likelihood is identical to the probability law of the

noise. For such experiments, Gull and Daniell [6] suggested the ME principle as appropriate to assign a probability distribution to any image along with a \mathbf{c}^2 -constraint for handling the errors e_m , $m = 1, 2, \dots, M$. The chi-squared distribution \mathbf{c}^2 , also called the statistical misfit, measures how well a model \mathbf{f} agrees with the measured data \mathbf{g}

$$\mathbf{c}^2(\mathbf{f}) = (\mathbf{g} - \mathbf{R}\mathbf{f})^T \mathbf{C}^{-1} (\mathbf{g} - \mathbf{R}\mathbf{f}) \quad (7)$$

An approximate equality holds if neglecting the off-diagonal covariances in \mathbf{C} , which is actually true if the noise is not correlated among pixels. Then the covariance matrix becomes diagonal and after a set of M measurements, the likelihood is

$$Pr(\mathbf{g}/\mathbf{f}/I) = \left[\prod_{m=1}^M (2p\mathbf{s}_m^2)^{-\frac{1}{2}} \right] \cdot \exp \left[-\frac{1}{2} \mathbf{c}^2(\mathbf{f}) \right] \quad (8)$$

where the squares of standard deviations are the diagonal covariances $\mathbf{s}_m^2 = C_{mm}$, $m = 1, 2, \dots, M$.

Solving the inverse problem of image restoration consists in choosing the optimal estimator $\tilde{\mathbf{f}}$ of the unknown function \mathbf{f} . This requires adopting an *estimation rule*, such as *posterior mean* or *maximum a posteriori* (MAP), in order to select an *optimal, unique and stable* solution. The power of the Bayesian approach lies in the steadfast use of the posterior probability. If we had to produce just one single image as the "best restoration", we would naturally give the *most probable* one that maximizes $Pr(\mathbf{f}/\mathbf{g}/I)$, along with some *statement of reliability* derived from the spread of all reasonably probable images. Bayesian approach aims to maximize the posterior probability $Pr(\mathbf{f}/\mathbf{g}/I)$ derived by replacing the prior (5) and the likelihood (8) in Bayes' theorem (6).

Consistent with the ME requirements, the Lagrangean associated with the MAP procedure must also contain the linear transform and the total flux constraints, which leads to the expression of the *potential function* Z of the image, which here is

$$Z(\mathbf{I}_1, \dots, \mathbf{I}_M, \mathbf{r}) = -U \cdot \ln \left[\sum_{n=1}^N \exp \left(-\sum_{m=1}^M \mathbf{I}_m R_{mn} \right) \right] - \frac{1}{4\mathbf{r}} \sum_{m=1}^M \mathbf{I}_m^2 \mathbf{s}_m^2 - \sum_{m=1}^M \mathbf{I}_m g_m + \mathbf{r}\mathbf{W} \quad (9)$$

where $\mathbf{I}_1, \mathbf{I}_2, \dots, \mathbf{I}_M, \mathbf{r}$ are the Lagrange multipliers and \mathbf{W} stands for the mean of the \mathbf{c}^2 function. Ultimately, the task reduces to finding the proper values of the Lagrange multipliers reaching the extremum of the potential function Z .

3 Results and Discussion

3.1 X-ray imaging

The production of X-ray images is heavily based on the assumption that the X-ray photons are passing through the imaged object along rectilinear paths. The *absorption* coefficient \mathbf{m} is defined by the rate of decreasing number N of recorded quanta $\frac{dN}{N} = -\mathbf{m} \cdot dx$. The total attenuation rate depends on the individual rates associated with all the interactions that may occur while the photons are passing through a sample. Assuming a homogeneous imaged object, we get the *attenuation equation* by integration of

$$\frac{N(E)}{N_0} = \exp(-\mathbf{m}(E) \cdot x) = \exp\left(-\frac{\mu}{\rho}(E) \cdot x\right) \quad (10)$$

The *mass attenuation* coefficient $\frac{\mathbf{m}}{\rho}$ depends on the material composition and the energy of the incident photons. We considered a simple approximation of the mass absorption coefficients for low Z matrices (sample) such as

$$\frac{\mathbf{m}}{\rho} = 2064 \cdot E^{-3.28} \bar{Z}^{4.62} + s_{KN}(E) \cdot \bar{Z} + 2.8 \cdot E^{-2.02} \cdot \bar{Z}^{4.86}$$

where $s_{KN}(E)$ is the Klein-Nishina cross section and \bar{Z} is the effective atomic number of the sample. Based on the above, the package GEANT 3.21 (<http://wwwinfo.cern.ch/asd/geant>) from CERN was used to simulate the average breast tissue scattering and to define the imaging system response.

3.2 Computational Aspects

The above derivation of the potential function Z is nevertheless effective *only* if reliable estimates of the noise standard deviations $s_m, m=1,2,\dots,M$ that determine the severity of blurring are *a priori* selected on some theoretical and/or experimental base. The major source of noise in X-ray imaging is the random distribution of photons over the surface of the image. The standard deviation of the photon concentrations is the best quantitative estimator of the noise in an image. Therefore, we set the standard deviation s_m in each pixel equal the square root of the recorded quanta g_m in agreement with Poisson's law

$$s_m = a\sqrt{g_m}, \quad m=1,2,\dots,M \quad (12)$$

The model parameter a sets down the proper

scattering range of the *signal-to-noise* ratios in each pixel around some common level and ensures convergence of the algorithm [12].

The minimization method of the potential function Z was based on Fletcher-Reeves' conjugate gradient algorithm for non-linear minimization with Polak-Ribière's ingredient for smoother transitions to further iterations required by not exactly quadratic forms. An original extension of Neville's algorithm for computing numerical derivatives was implemented to provide gradient information for any given functional procedure. The algorithm was implemented in MS Visual C++ and run on purpose under Windows 95 on a low-priced PC Pentium III. Processing time of 512×512 pixel size images was in the range of 1 to 2 minutes, significantly depending on the texture richness. Pixel depth was set to 8 bits. LView Pro 1.D2/32 freeware software was used for graphics file format conversions, image display, and file import-export.

3.3 Image Processing

In order to ensure algorithm convergence, we simulated various opacities embedded in breast-like tissue (Fig. 1) and set the value of our model parameter for achieving the best restoration of the simulated opacities. Tests were carried out on both optically scanned X-ray mammograms and samples from various databases available on the web.

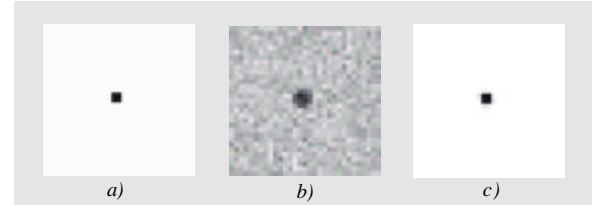


Fig.1 Simulated microcalcification of 2×2 pixel size embedded in a homogeneous mammalian-like tissue; a) simulated microcalcification, b) simulated tissue including the microcalcification, c) microcalcification image after the restoration process.

Some clinically relevant digital restorations of raw X-ray images are presented in Fig. 2. The main steps in our tests focused on detecting false positives are displayed in Fig. 3. Quality assessment was performed on the basis of Contrast-Detail (CD) phantoms as fostered by the University Hospital in Nijmegen [13]. There were detected neither spurious patterns nor any suspect forms.

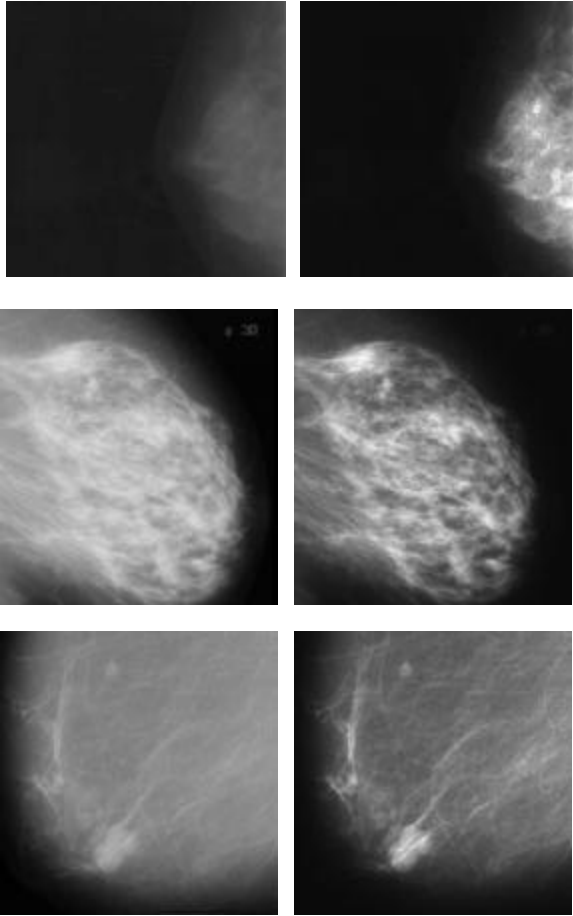


Fig. 2 Full breast mammograms; *left column*: raw digitized X-ray images by optical scanning; *right column*: digitally restored images; *top*: Fundeni Hospital, Romania (<http://fipce4.fizica.unibuc.ro>) - normal breast; *middle*: Case *mdb032*, MIAS, UK (<http://marathon.csee.usf.edu/>) - benign ill-defined masses, fatty-glandular tissue; *bottom*: Case *mdb005*, MIAS - benign circumscribed masses - fatty tissue.

4. Conclusion

Our approach highlighted the power of ME methods in solving the inverse problem of digital image restoration in the framework of Bayesian statistics. Whether it might be for spectral analysis of time series, radio astronomy, optical X-ray astronomy and tomography, or for any reconstruction of positive, additive images, the ME principle assigns a prior probability in Bayesian sense to a given image.

Theoretically, no artifacts should pop up after data processing, since the entropy maximization produces the most unbiased and featureless solution, which is consistent with the data and complies with the errors in measurements and modeling.

The algorithm developed may apply to virtually

any type of data assuming that the PSF of the measuring equipment is adequately known and a χ^2 - constraint for the errors in the input data holds reasonably.

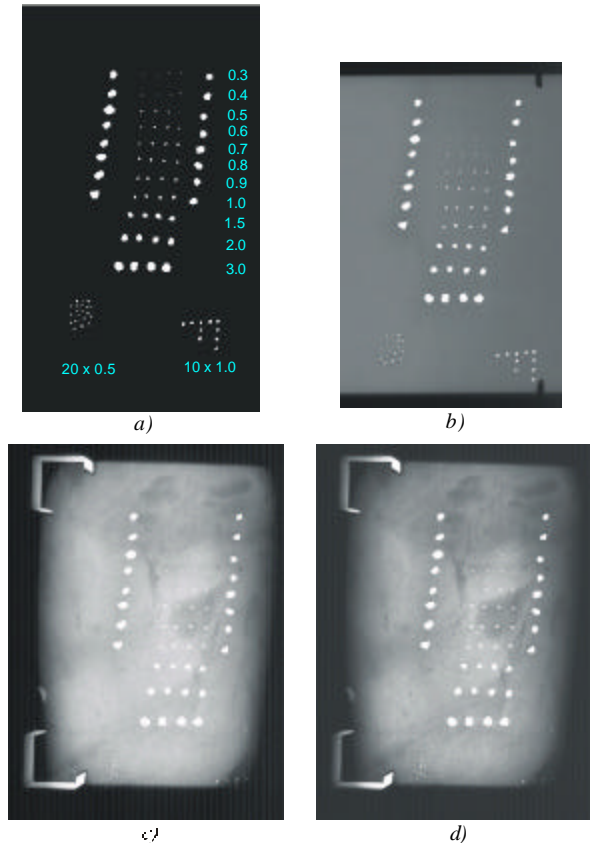


Fig. 3 Test pattern for detecting artifacts in mammalian-like tissue (average diameters of grains in millimeters);

- arrangement of various size marble grains;
- X-ray image of the grains;
- X-ray image of the grains embedded in the tissue;
- Image c) after the restoration process.

Acknowledgments

R.M. is supported by a postdoc grant from the European Community, FP5 (QLG3-CT-2000-30161). M.M.V.H. is supported by research grants received from the Fund for Scientific Research (G.0185.96N), the National Lottery (Belgium) (9.0185.96), the Flemish Regional Ministry of Education (Belgium) (GOA 95/99-06; 2000/11), the Flemish Ministry for Science and Technology (VIS/98/012), and the European Community, FP5 (QLG3-CT-2000-30161 and IST-2001-32114). R.M. is grateful to A.M.- Djafari for his prompt and efficient support.

References:

- [1] S. Mallat, A theory for multiresolution signal decomposition: The wavelet representation, *IEEE Trans.*, Vol. PAMI-11, No 7, 1989, pp. 674-693.
- [2] Y. Meyer, Review of an introduction to wavelets and ten lectures on wavelets, *Bull. Amer Math. Soc.*, Vol. 28, 1993, pp. 350-359.
- [3] D.L. Donoho, Unconditional bases and bit-level compression, *Appl. Comput. Harmonic Anal.*, Vol. 1, No. 1, 1996, pp. 100-105.
- [4] E.J. Candes, Ridgelets: Theory and Applications, *Ph.D. Thesis*, Department of Statistics, Stanford University, USA, 1998.
- [5] G.J. Daniell, Of maps and monkeys: An introduction to the Maximum Entropy Method, in *Maximum Entropy in Action* (B. Buck and V.A. Macaulay, Eds.), Clarendon Press, Oxford, 1994, pp. 1-18.
- [6] S.F. Gull, G.J. Daniell, (1978) Image reconstruction from incomplete and noisy data. *Nature*, Vol. 272, 1978, pp. 686-690.
- [7] J. Skilling, Fundamentals of MaxEnt in data analysis, in *Maximum Entropy in Action* (B. Buck and V.A. Macaulay, Eds.), Clarendon Press, Oxford, 1994, pp. 19-40.
- [8] A.M.-Djafari, Maximum entropy and linear inverse problems, in *Maximum Entropy and Bayesian Methods* (A.M.-Djafari and G. Demoment, Eds.), Kluwer Academic Publishers, Amsterdam, 1993, pp. 253-264.
- [9] M.Z. Nashed, Operator-theoretic and computational approaches to ill-posed problems with applications to antenna theory, *IEEE Trans. Antennas Propagat*, Vol. 29, 1981, pp. 220-231.
- [10] M.K. Hanson, Bayesian and related methods in image reconstruction from incomplete data, in *Image Recovery: Theory and Application* (H. Stark, Ed.), Academic Press, Orlando, 1987.
- [11] C.E. Shannon, A mathematical theory of communication, *Bell, Syst. Tech. J.*, Vol. 27, 1948, pp. 379-423.
- [12] R. Mutihac, A.A. Colavita, A. Cicuttin, A. Cerdeira, Maximum entropy improvement of X-ray digital mammograms", *Digital Mammography* (N. Karssemeijer, M. Thijssen, J. Hendriks, and L. van Erning, Eds.), *Image Processing and Display*, Kluwer Academic Publishers, Dordrecht, 1998, pp. 329-337.
- [13] M.A.O. Thijsen, K.R. Bijkerk, and R.J.M. van der Burght, *Manual CDRAD-phantom type 2.0*, Department of Radiology, University Hospital Nijmegen, St. Radboud, NL-6500 HB Nijmegen, The Netherlands, 1992.